DESY-09-072
June 2009

Multi-lepton production at high transverse momentum at HERA

ZEUS Collaboration

Abstract

A search for events containing two or more high-transverse-momentum isolated leptons has been performed in ep collisions with the ZEUS detector at HERA using the full collected data sample, corresponding to an integrated luminosity of $480\,\mathrm{pb}^{-1}$. The number of observed events has been compared with the prediction from the Standard Model, searching for possible deviations, especially for multi-lepton events with invariant mass larger than 100 GeV. Good agreement with the Standard Model has been observed. Total and differential cross sections for di-lepton production have been measured in a restricted phase space dominated by photon-photon collisions.

The ZEUS Collaboration

S. Chekanov, M. Derrick, S. Magill, B. Musgrave, D. Nicholass[1], J. Repond, R. Yoshida
Argonne National Laboratory, Argonne, Illinois 60439-4815, USA [n]

M.C.K. Mattingly
Andrews University, Berrien Springs, Michigan 49104-0380, USA

P. Antonioli, G. Bari, L. Bellagamba, D. Boscherini, A. Bruni, G. Bruni, F. Cindolo, M. Corradi, G. Iacobucci, A. Margotti, R. Nania, A. Polini
INFN Bologna, Bologna, Italy [e]

S. Antonelli, M. Basile, M. Bindi, L. Cifarelli, A. Contin, S. De Pasquale[2], G. Sartorelli, A. Zichichi
University and INFN Bologna, Bologna, Italy [e]

D. Bartsch, I. Brock, H. Hartmann, E. Hilger, H.-P. Jakob, M. Jüngst, A.E. Nuncio-Quiroz, E. Paul, U. Samson, V. Schönberg, R. Shehzadi, M. Wlasenko
Physikalisches Institut der Universität Bonn, Bonn, Germany [b]

J.D. Morris[3]
H.H. Wills Physics Laboratory, University of Bristol, Bristol, United Kingdom [m]

M. Kaur, P. Kaur[4], I. Singh[4]
Panjab University, Department of Physics, Chandigarh, India

M. Capua, S. Fazio, A. Mastroberardino, M. Schioppa, G. Susinno, E. Tassi
Calabria University, Physics Department and INFN, Cosenza, Italy [e]

J.Y. Kim
Chonnam National University, Kwangju, South Korea

Z.A. Ibrahim, F. Mohamad Idris, B. Kamaluddin, W.A.T. Wan Abdullah
Jabatan Fizik, Universiti Malaya, 50603 Kuala Lumpur, Malaysia [r]

Y. Ning, Z. Ren, F. Sciulli
Nevis Laboratories, Columbia University, Irvington on Hudson, New York 10027, USA [o]

J. Chwastowski, A. Eskreys, J. Figiel, A. Galas, K. Olkiewicz, B. Pawlik, P. Stopa, L. Zawiejski
The Henryk Niewodniczanski Institute of Nuclear Physics, Polish Academy of Sciences, Cracow, Poland [i]

L. Adamczyk, T. Bołd, I. Grabowska-Bołd, D. Kisielewska, J. Łukasik[5], M. Przybycień, L. Suszycki
Faculty of Physics and Applied Computer Science, AGH-University of Science and Technology, Cracow, Poland [p]

A. Kotański[6], W. Słomiński[7]
Department of Physics, Jagellonian University, Cracow, Poland

O. Behnke, J. Behr, U. Behrens, C. Blohm, K. Borras, D. Bot, R. Ciesielski, N. Coppola, S. Fang, A. Geiser, P. Göttlicher[8], J. Grebenyuk, I. Gregor, T. Haas, W. Hain, A. Hüttmann, F. Januschek, B. Kahle, I.I. Katkov[9], U. Klein[10], U. Kötz, H. Kowalski, M. Lisovyi, E. Lobodzinska, B. Löhr, R. Mankel[11], I.-A. Melzer-Pellmann, S. Miglioranzi[12], A. Montanari, T. Namsoo, D. Notz, A. Parenti, P. Roloff, I. Rubinsky, U. Schneekloth, A. Spiridonov[13], D. Szuba[14], J. Szuba[15], T. Theedt, J. Tomaszewska[16], G. Wolf, K. Wrona, A.G. Yagües-Molina, C. Youngman, W. Zeuner[11]
Deutsches Elektronen-Synchrotron DESY, Hamburg, Germany

V. Drugakov, W. Lohmann, S. Schlenstedt
Deutsches Elektronen-Synchrotron DESY, Zeuthen, Germany

G. Barbagli, E. Gallo
INFN Florence, Florence, Italy [e]

P. G. Pelfer
University and INFN Florence, Florence, Italy [e]

A. Bamberger, D. Dobur, F. Karstens, N.N. Vlasov[17]
Fakultät für Physik der Universität Freiburg i.Br., Freiburg i.Br., Germany [b]

P.J. Bussey, A.T. Doyle, M. Forrest, D.H. Saxon, I.O. Skillicorn
Department of Physics and Astronomy, University of Glasgow, Glasgow, United Kingdom [m]

I. Gialas[18], K. Papageorgiu
Department of Engineering in Management and Finance, Univ. of the Aegean, Chios, Greece

U. Holm, R. Klanner, E. Lohrmann, H. Perrey, P. Schleper, T. Schörner-Sadenius, J. Sztuk, H. Stadie, M. Turcato
Hamburg University, Institute of Exp. Physics, Hamburg, Germany [b]

K.R. Long, A.D. Tapper
Imperial College London, High Energy Nuclear Physics Group, London, United Kingdom [m]

T. Matsumoto, K. Nagano, K. Tokushuku[19], S. Yamada, Y. Yamazaki[20]
Institute of Particle and Nuclear Studies, KEK, Tsukuba, Japan [f]

A.N. Barakbaev, E.G. Boos, N.S. Pokrovskiy, B.O. Zhautykov
Institute of Physics and Technology of Ministry of Education and Science of Kazakhstan, Almaty, Kazakhstan

V. Aushev[21], O. Bachynska, M. Borodin, I. Kadenko, O. Kuprash, V. Libov, D. Lontkovskyi, I. Makarenko, Iu. Sorokin, A. Verbytskyi, O. Volynets, M. Zolko
Institute for Nuclear Research, National Academy of Sciences, and Kiev National University, Kiev, Ukraine

D. Son
Kyungpook National University, Center for High Energy Physics, Daegu, South Korea [g]

J. de Favereau, K. Piotrzkowski
Institut de Physique Nucléaire, Université Catholique de Louvain, Louvain-la-Neuve, Belgium [q]

F. Barreiro, C. Glasman, M. Jimenez, J. del Peso, E. Ron, J. Terrón, C. Uribe-Estrada
Departamento de Física Teórica, Universidad Autónoma de Madrid, Madrid, Spain [l]

F. Corriveau, J. Schwartz, C. Zhou
Department of Physics, McGill University, Montréal, Québec, Canada H3A 2T8 [a]

T. Tsurugai
Meiji Gakuin University, Faculty of General Education, Yokohama, Japan [f]

A. Antonov, B.A. Dolgoshein, D. Gladkov, V. Sosnovtsev, A. Stifutkin, S. Suchkov
Moscow Engineering Physics Institute, Moscow, Russia [j]

R.K. Dementiev, P.F. Ermolov †, L.K. Gladilin, Yu.A. Golubkov, L.A. Khein, I.A. Korzhavina, V.A. Kuzmin, B.B. Levchenko[22], O.Yu. Lukina, A.S. Proskuryakov, L.M. Shcheglova, D.S. Zotkin
Moscow State University, Institute of Nuclear Physics, Moscow, Russia [k]

I. Abt, A. Caldwell, D. Kollar, B. Reisert, W.B. Schmidke
Max-Planck-Institut für Physik, München, Germany

G. Grigorescu, A. Keramidas, E. Koffeman, P. Kooijman, A. Pellegrino, H. Tiecke, M. Vázquez[12], L. Wiggers
NIKHEF and University of Amsterdam, Amsterdam, Netherlands [h]

N. Brümmer, B. Bylsma, L.S. Durkin, A. Lee, T.Y. Ling
Physics Department, Ohio State University, Columbus, Ohio 43210, USA [n]

A.M. Cooper-Sarkar, R.C.E. Devenish, J. Ferrando, B. Foster, C. Gwenlan[23], K. Horton[24], K. Oliver, A. Robertson, R. Walczak
Department of Physics, University of Oxford, Oxford United Kingdom [m]

A. Bertolin, F. Dal Corso, S. Dusini, A. Longhin, L. Stanco
INFN Padova, Padova, Italy [e]

R. Brugnera, R. Carlin, A. Garfagnini, S. Limentani
Dipartimento di Fisica dell' Università and INFN, Padova, Italy [e]

B.Y. Oh, A. Raval, J.J. Whitmore[25]
Department of Physics, Pennsylvania State University, University Park, Pennsylvania 16802, USA [o]

Y. Iga
Polytechnic University, Sagamihara, Japan [f]

G. D'Agostini, G. Marini, A. Nigro
Dipartimento di Fisica, Università 'La Sapienza' and INFN, Rome, Italy [e]

J.C. Hart
Rutherford Appleton Laboratory, Chilton, Didcot, Oxon, United Kingdom [m]

H. Abramowicz[26], R. Ingbir, S. Kananov, A. Levy, A. Stern
Raymond and Beverly Sackler Faculty of Exact Sciences, School of Physics, Tel Aviv University,
Tel Aviv, Israel [d]

M. Ishitsuka, T. Kanno, M. Kuze, J. Maeda
Department of Physics, Tokyo Institute of Technology, Tokyo, Japan [f]

R. Hori, S. Kagawa[27], N. Okazaki, S. Shimizu, T. Tawara
Department of Physics, University of Tokyo, Tokyo, Japan [f]

R. Hamatsu, H. Kaji[28], S. Kitamura[29], O. Ota[30], Y.D. Ri
Tokyo Metropolitan University, Department of Physics, Tokyo, Japan [f]

M. Costa, M.I. Ferrero, V. Monaco, R. Sacchi, V. Sola, A. Solano
Università di Torino and INFN, Torino, Italy [e]

M. Arneodo, M. Ruspa
Università del Piemonte Orientale, Novara, and INFN, Torino, Italy [e]

S. Fourletov[31], J.F. Martin, T.P. Stewart
Department of Physics, University of Toronto, Toronto, Ontario, Canada M5S 1A7 [a]

S.K. Boutle[18], J.M. Butterworth, T.W. Jones, J.H. Loizides, M. Wing[32]
Physics and Astronomy Department, University College London, London, United Kingdom [m]

B. Brzozowska, J. Ciborowski[33], G. Grzelak, P. Kulinski, P. Łużniak[34], J. Malka[34], R.J. Nowak, J.M. Pawlak, W. Perlanski[34], A.F. Żarnecki
Warsaw University, Institute of Experimental Physics, Warsaw, Poland

M. Adamus, P. Plucinski[35], T. Tymieniecka
Institute for Nuclear Studies, Warsaw, Poland

Y. Eisenberg, D. Hochman, U. Karshon
Department of Particle Physics, Weizmann Institute, Rehovot, Israel [c]

E. Brownson, D.D. Reeder, A.A. Savin, W.H. Smith, H. Wolfe
Department of Physics, University of Wisconsin, Madison, Wisconsin 53706, USA [n]

S. Bhadra, C.D. Catterall, G. Hartner, U. Noor, J. Whyte
Department of Physics, York University, Ontario, Canada M3J 1P3 [a]

[1] also affiliated with University College London, United Kingdom
[2] now at University of Salerno, Italy
[3] now at Queen Mary University of London, United Kingdom
[4] also working at Max Planck Institute, Munich, Germany
[5] now at Institute of Aviation, Warsaw, Poland
[6] supported by the research grant No. 1 P03B 04529 (2005-2008)
[7] This work was supported in part by the Marie Curie Actions Transfer of Knowledge project COCOS (contract MTKD-CT-2004-517186)
[8] now at DESY group FEB, Hamburg, Germany
[9] also at Moscow State University, Russia
[10] now at University of Liverpool, United Kingdom
[11] on leave of absence at CERN, Geneva, Switzerland
[12] now at CERN, Geneva, Switzerland
[13] also at Institut of Theoretical and Experimental Physics, Moscow, Russia
[14] also at INP, Cracow, Poland
[15] also at FPACS, AGH-UST, Cracow, Poland
[16] partially supported by Warsaw University, Poland
[17] partially supported by Moscow State University, Russia
[18] also affiliated with DESY, Germany
[19] also at University of Tokyo, Japan
[20] now at Kobe University, Japan
[21] supported by DESY, Germany
[22] partially supported by Russian Foundation for Basic Research grant No. 05-02-39028-NSFC-a
[23] STFC Advanced Fellow
[24] nee Korcsak-Gorzo
[25] This material was based on work supported by the National Science Foundation, while working at the Foundation.
[26] also at Max Planck Institute, Munich, Germany, Alexander von Humboldt Research Award
[27] now at KEK, Tsukuba, Japan
[28] now at Nagoya University, Japan
[29] member of Department of Radiological Science, Tokyo Metropolitan University, Japan
[30] now at SunMelx Co. Ltd., Tokyo, Japan
[31] now at University of Bonn, Germany
[32] also at Hamburg University, Inst. of Exp. Physics, Alexander von Humboldt Research Award and partially supported by DESY, Hamburg, Germany
[33] also at Łódź University, Poland
[34] member of Łódź University, Poland
[35] now at Lund University, Lund, Sweden
[†] deceased

[a] supported by the Natural Sciences and Engineering Research Council of Canada (NSERC)

[b] supported by the German Federal Ministry for Education and Research (BMBF), under contract Nos. 05 HZ6PDA, 05 HZ6GUA, 05 HZ6VFA and 05 HZ4KHA

[c] supported in part by the MINERVA Gesellschaft für Forschung GmbH, the Israel Science Foundation (grant No. 293/02-11.2) and the US-Israel Binational Science Foundation

[d] supported by the Israel Science Foundation

[e] supported by the Italian National Institute for Nuclear Physics (INFN)

[f] supported by the Japanese Ministry of Education, Culture, Sports, Science and Technology (MEXT) and its grants for Scientific Research

[g] supported by the Korean Ministry of Education and Korea Science and Engineering Foundation

[h] supported by the Netherlands Foundation for Research on Matter (FOM)

[i] supported by the Polish State Committee for Scientific Research, project No. DESY/256/2006 - 154/DES/2006/03

[j] partially supported by the German Federal Ministry for Education and Research (BMBF)

[k] supported by RF Presidential grant N 1456.2008.2 for the leading scientific schools and by the Russian Ministry of Education and Science through its grant for Scientific Research on High Energy Physics

[l] supported by the Spanish Ministry of Education and Science through funds provided by CICYT

[m] supported by the Science and Technology Facilities Council, UK

[n] supported by the US Department of Energy

[o] supported by the US National Science Foundation. Any opinion, findings and conclusions or recommendations expressed in this material are those of the authors and do not necessarily reflect the views of the National Science Foundation.

[p] supported by the Polish Ministry of Science and Higher Education as a scientific project (2009-2010)

[q] supported by FNRS and its associated funds (IISN and FRIA) and by an Inter-University Attraction Poles Programme subsidised by the Belgian Federal Science Policy Office

[r] supported by an FRGS grant from the Malaysian government

1 Introduction

The production of multi-lepton final states in electron-proton collisions[1] is predicted within the framework of the Standard Model (SM). At HERA energies, the production cross sections are small for high transverse momenta, p_T, of the produced leptons and, along with the distributions of the kinematic quantities, can be calculated with high accuracy in the SM. Therefore contributions from beyond the SM could either be observed as an increase of the visible cross sections or as a deviation from the predicted distributions.

Multi-lepton final states were searched for by the H1 Collaboration [1] using a luminosity of $463\,\mathrm{pb}^{-1}$. The observed overall numbers of di- and tri-lepton events were in good agreement with the SM predictions. However, some events with large transverse momenta were observed, exceeding SM predictions in this region.

The analysis presented here is based on a luminosity of $480\,\mathrm{pb}^{-1}$ collected by the ZEUS experiment. Events with two or more high-p_T leptons (electrons or muons) were searched for and the total yields and distributions of kinematic variables were compared to SM predictions. In addition, the total visible and differential cross sections for di-lepton production were measured in the photoproduction regime, in which the incoming electron has small squared momentum transfer, $Q^2 < 1\,\mathrm{GeV}^2$.

2 Experimental set-up

The analysed data were collected between 1996 and 2007 at the electron-proton collider HERA using the ZEUS detector. During this period HERA operated with an electron beam energy of 27.5 GeV and a proton beam energy of 820 GeV and, from 1998, of 920 GeV, corresponding to centre-of-mass energies of 300 GeV and 318 GeV, respectively.

A detailed description of the ZEUS detector can be found elsewhere [2]. A brief outline of the components that are most relevant for this analysis is given below.

Charged particles were tracked in the central tracking detector (CTD) [3], which operated in a magnetic field of 1.43 T provided by a thin superconducting solenoid and covered the polar-angle[2] region $15^\circ < \theta < 164^\circ$. Before the 2003–2007 running period, the ZEUS

[1] Here and in the following, the term "electron" denotes generically both the electron (e^-) and the positron (e^+).

[2] The ZEUS coordinate system is a right-handed Cartesian system, with the Z axis pointing in the proton beam direction, the Y axis pointing up and the X axis pointing towards the centre of HERA. The polar angle, θ, is measured with respect to the proton beam direction. The coordinate origin is at the nominal interaction point.

tracking system was upgraded with a silicon microvertex detector (MVD) [4]. The high-resolution uranium–scintillator calorimeter (CAL) [5] consisted of three parts: the forward (FCAL), the barrel (BCAL) and the rear (RCAL) calorimeters. The smallest subdivision of the CAL was called a cell. The muon system consisted of rear, barrel (R/BMUON) [6] and forward (FMUON) [2] tracking detectors. The B/RMUON consisted of limited-streamer (LS) tube chambers placed behind the BCAL (RCAL), inside and outside a magnetised iron yoke surrounding the CAL. The barrel and rear muon chambers covered polar angles from 34° to 135° and from 135° to 171°, respectively. The FMUON consisted of six trigger planes of LS tubes and four planes of drift chambers covering the angular region from 5° to 32°. The muon system exploited the magnetic field of the iron yoke and, in the forward direction, of two iron toroids magnetised to $\sim 1.6\,\mathrm{T}$ to provide a measurement of the muon momentum.

The luminosity was measured using the Bethe-Heitler reaction $ep \to e\gamma p$ by a luminosity detector which consisted of a lead–scintillator [7–9] calorimeter and, in the 2003–07 running period, an independent magnetic spectrometer [10]. The fractional systematic uncertainty on the measured luminosity was 2.5%.

The integrated luminosity of the samples corresponds to $480\,\mathrm{pb}^{-1}$ for events in which a search of electrons but no muons was carried out (electron channel) and to $444\,\mathrm{pb}^{-1}$ for events in which a search for either muons or electrons was carried out (muon channel). The slight difference in integrated luminosity is due to the requirement of a good performance of the detector components involved in the search.

3 Standard Model processes and Monte Carlo simulation

To evaluate the detector acceptance and to provide simulations of signal and background distributions, Monte Carlo (MC) samples of signal and background events were generated.

The SM predicts that isolated multi-lepton final states are predominantly produced by two-photon interactions, $\gamma\gamma \to l^+l^-$. The GRAPE MC event generator [11] was used to simulate these processes. It also includes contributions from γZ and ZZ interactions, photon internal conversions and virtual and real Z production. It is based on the electroweak matrix elements at tree level. At the proton vertex, three contributions were considered: elastic, where the proton stays intact; quasi-elastic, where a resonant state is formed; and inelastic, where the proton interacts via its quark constituents. At the electron vertex, all values of Q^2 were generated, from $Q^2 \simeq 0$ GeV^2 (photoproduction) to the deep inelastic scattering (DIS) regime. The uncertainty on the GRAPE predictions

was taken to be 3% [1].

The Drell-Yan process from resolved photon events, in which the photon fluctuates into a $q\bar{q}$ pair, and the lepton pair is produced from the interaction between a quark in the proton and one of the quarks from the photon, is not included. However this is expected to be negligible in the investigated kinematic regime [12].

The dominant SM background to topologies in which at least one electron is identified comes from neutral current (NC) DIS and QED Compton (QEDC) events. In NC ($ep \to eX$) events, the scattered electron is identified as one of the electrons of the pair and hadrons or photons in the hadronic system X are misidentified as a further electron. In QEDC events ($ep \to e\gamma X$), the final-state photon may convert into an e^+e^- pair in the detector material in front of the CTD and typically one of these two electrons is identified as the second electron of the pair.

The NC DIS and QEDC events were simulated with the DJANGOH [13] and GRAPE-COMPTON [11] MC programs, respectively. The absolute predictions of the GRAPE-COMPTON MC were scaled by a factor 1.13 in order to correct imperfections in the simulation of the dead material between the beampipe and the CTD. The uncertainty on this factor was taken as a source of systematic uncertainty. For the final-state topologies in which an electron and a muon were found, the background from SM di-tau pair production was estimated using the GRAPE MC program.

Standard Model processes such as vector-meson (Υ, charmonium) and open heavy-flavour (charm and beauty) production were studied using the DIFFVM [14] and PYTHIA [15] MC programs and were found to be negligible.

The generated events were passed through a full simulation of the ZEUS detector based on the GEANT [16] program versions 3.13 (1996–2000) and 3.21 (2003–07). They were then subjected to the same trigger requirements and processed by the same reconstruction program as the data.

4 Event selection

4.1 Online selection

Events with two or more leptons in the final state were selected using the ZEUS three-level trigger system [2, 17, 18].

To select electrons, a significant energy deposit was required in the electromagnetic calorimeter and at least one good track in the central detectors had to be present. In addition, two other trigger chains were used: the first, dedicated to NC DIS selection,

requiring the detection of an electron with an energy $E'_e > 4\,\text{GeV}$; the second, dedicated to the selection of events with high transverse energy deposited in the calorimeter ($E_T > 25\,\text{GeV}$).

To select muons [19], a candidate was identified as a central track measured in the CTD matched to an energy deposit in the CAL and to a segment in the barrel or rear inner muon chambers.

4.2 Electron identification

The following criteria were imposed to select electrons in the offline analysis:

- electron identification — an algorithm [20] which combined information from the energy deposits in the calorimeter and, when available, tracks measured in the central tracking detectors was used to identify the electron candidates. Electron candidates in the central region ($20^\circ < \theta^e < 150^\circ$) were required to have energy greater than 10 GeV and a track matched with the energy deposit in the calorimeter. The matched track was required to be fitted to the primary vertex and to have a momentum of at least 3 GeV and a distance of closest approach between the energy deposition and the track of less than 8 cm. Forward electrons ($5^\circ < \theta^e < 20^\circ$) were also required to have an energy greater than 10 GeV while, for electrons in the rear region ($150^\circ < \theta^e < 175^\circ$), the energy requirement was decreased to 5 GeV;
- isolation — to ensure high purity, each electron candidate was required to be isolated such that the total energy not associated with the electron in an $\eta-\phi$ cone of radius 0.8 centred on the electron was less than 0.3 GeV. This requirement was complemented, for electrons in the central region, by the request that no track with $p_T > 1\,\text{GeV}$, other than the matching track, was contained in an $\eta - \phi$ cone of radius 0.4 centred on the electron;
- QEDC background reduction — for the data collected in 2003–07, each track associated with an electron candidate was required to have at least two hits in the MVD. This requirement removed photon conversions in the material between the MVD and the CTD.

4.3 Muon identification

The following criteria were imposed to select muons in the offline analysis:

- muon identification — at least one muon candidate in the event was required to be reconstructed by the rear, barrel or forward muon chambers, matched to a track and to

an energy deposit in the calorimeter. In the case when only one muon in the event was reconstructed by the muon chambers, additional muons were also selected with looser criteria, by requiring a track pointing towards a calorimeter energy deposit compatible with that from a minimum ionising particle (mip). Each muon candidate was required to be associated with a track fitted to the primary vertex. The muon momentum was reconstructed using the central tracking devices, complemented with the information from the FMUON when available. The muon was required to have $p_T^\mu > 2\,\mathrm{GeV}$, and to lie in the angular region $20^\circ < \theta^\mu < 26^\circ$ (FMUON), $35^\circ < \theta^\mu < 160^\circ$ (B/RMUON), $20^\circ < \theta^\mu < 160^\circ$ (mip);

- isolation — to ensure high purity, each identified muon was required to be isolated such that only the matching track was contained in an $\eta - \phi$ cone of radius 1.0 centred on the muon. This cut, harder than in the electron selection, was used to reject background events in which a muon was found very close to a hadronic system, in particular in the $e\mu$ channel;
- cosmic-muon background reduction — the reconstructed primary vertex had to be consistent with the HERA beam-spot position. If two muons were found, the acollinearity angle, Ω, between the two muons had to satisfy $\cos\Omega > -0.995$. For events with $\cos\Omega < -0.990$, additional CAL timing cuts were applied.

4.4 Event selection and classification

The final event selection required the event vertex to be reconstructed with $|Z_{\mathrm{VTX}}| < 30\,\mathrm{cm}$. At least two leptons, electrons or muons, had to be reconstructed in the central part of the detector ($20^\circ < \theta^l < 150^\circ$). One of the leptons had to have $p_T^{l_1} > 10\,\mathrm{GeV}$ and the other $p_T^{l_2} > 5\,\mathrm{GeV}$. Additional leptons identified as described in Sections 4.2 and 4.3 could be present in the event. No explicit requirement on the charge of the leptons was imposed. According to the number and the flavour of the lepton candidates, the events were classified into mutually exclusive samples.

For the measurement of the production cross section of e^+e^- and $\mu^+\mu^-$ pairs in the photoproduction regime, the cut $(E - P_Z) < 45\,\mathrm{GeV}$ was applied. This quantity was reconstructed in the electron case as

$$E - P_Z = \sum_i E_i^{\mathrm{corr}}(1 - \cos(\theta_i)), \tag{1}$$

where the sum runs over the corrected energies, E_i^{corr}, of the CAL clusters and, in the muon case, as

$$E - P_Z = \sum_i E_i(1 - \cos(\theta_i)) - \sum_{\mathrm{mip}} E_{\mathrm{mip}}(1 - \cos(\theta_{\mathrm{mip}})) + \sum_{\mathrm{muon}} E_{\mathrm{muon}}(1 - \cos(\theta_{\mathrm{muon}})), \tag{2}$$

where E_i is the energy of the i^{th} CAL cell and the $(E-P_Z)$ of the CAL mip was replaced by that of the muon track. This requirement selects events in which the scattered electron was lost in the beampipe and corresponds to a cut of $Q^2 < 1\,\text{GeV}^2$ and on the event inelasticity, $y = (E - P_Z)/2E_e < 0.82$, where E_e is the electron beam energy. The background from NC DIS and QEDC events is negligible in this sample, which will be referred to as the $\gamma\gamma$ sample in the following.

5 Systematic uncertainties

The following sources of systematic uncertainties were considered; the effect on the total visible cross section is given:

- the muon acceptance, including the B/RMUON trigger, the reconstruction and the muon identification efficiencies, is known to about 7% from a study based on an independent elastic di-muon sample [21], resulting in an uncertainty of $(^{+10\%}_{-8\%})$ for muons;
- the uncertainty on the efficiency of the CTD part of the trigger chain was estimated from a study based on an independent sample of low-multiplicity low-Q^2 DIS events [22], resulting in an uncertainty of +5% for electrons and ±5% for muons;
- the CAL energy scale was varied by its uncertainty of 3%, resulting in an uncertainty of $(^{+4\%}_{-3\%})$ for electrons and negligible for muons;
- the uncertainty on the efficiency of the CAL part of the muon trigger (±3%) and of the mip finder (±2%) resulted in an uncertainty of ±4% for muons;
- the uncertainty on the measurement of the hadronic system was evaluated by using an alternative reconstruction of $E-P_Z$, resulting in an uncertainty of −1.8% for electrons;
- the scaling factor of the QEDC MC was varied between 0.95 and 1.31, as allowed by the comparison with a QEDC-enriched data sample, resulting in a negligible effect for both electrons and muons.

The total systematic uncertainty was obtained by adding the individual contributions in quadrature. A 2.5% overall normalisation uncertainty associated with the luminosity measurement was included only in the systematic uncertainty of the total visible cross section.

6 Results

The number of selected events in the data are compared to SM predictions in Table 1. The following different di- and tri-lepton topologies are listed: ee, $\mu\mu$, $e\mu$, eee and $e\mu\mu$. The observed number of events is in good agreement with the predictions of the SM, according to which the NC DIS and QEDC processes give a sizeable contribution to the ee channel. Most of the events contributing to the $e\mu$ topology are predicted to come from di-muon production at high Q^2, in which the beam electron is scattered at large angles and is therefore seen in the detector, while one of the muons is outside the acceptance region. A small contribution to this channel (~ 2 events) is predicted to come from di-τ production, while the NC DIS background constitutes $\sim 10\%$ of the sample.

Three four-lepton events, 2 in the $ee\mu\mu$ and 1 in the $eeee$ channel, were observed, to be compared to a SM expectation of ~ 1. The contributions from true four-lepton events are not included in the SM predictions and are expected to be small. Events with other multi-lepton topologies were searched for, but none was found.

In Tables 1 and 2 the NC DIS and QEDC background contributions are given as limits at 95% confidence level (C.L.) when none or few events were selected from the background MC samples. When this is done, the central value of the total SM prediction is determined as the most probable value (mode) of the convolution of the Gaussian signal distribution with the poissonian background distributions, and the uncertainty on the total SM prediction is determined by taking the 68% C.L. interval.

Two events, one with three electrons in the final state and one with two muons and an electron, passing the three-lepton selection cuts, are shown in Fig. 1.

6.1 Kinematic distributions

The distributions of the mass of the two highest-p_T leptons in the event, M_{12}, and of the scalar sum of the transverse momenta of all the identified leptons in the event, $\sum p_T^l$, are shown in Figs. 2 and 3 for all the observed di- and tri-lepton topologies, and are compared to SM predictions. The SM gives a good description of the data. In the mass region between 80 and 100 GeV, which is sensitive to Z^0 production, 7 events were observed in the data, compatible with the predictions from the SM of ~ 9 events, including ~ 1 event from real Z^0 production.

The high-mass and high-$\sum p_T^l$ regions are particularly sensitive to possible contributions from physics beyond the SM. The event yields for $M_{12} > 100$ GeV for all the observed di- and tri-lepton channels are summarised in Table 2. In the electron channels, 3 events at high masses are observed, to be compared with a SM prediction of 2.5. Two of these

events are observed in the *eee* topology, for which the SM expectation is 0.7. No event with $M_{12} > 100$ GeV is seen in the muon channels. The event yield for $\sum p_T^l > 100\,\mathrm{GeV}$, combined for all the lepton topologies, is summarised in Table 3. Two events at high-$\sum p_T^l$ are observed, to be compared with a SM prediction of ~ 1.6.

The distributions of M_{12} and $\sum p_T^l$, combined for all the di- and tri-lepton topologies, are shown in Fig. 4. Also in this case, the data are well described by the SM predictions.

6.2 Cross sections

Total visible and differential cross sections for di-electron and di-muon production were determined in the kinematic region defined by:

$$p_T^{l_1} > 10\,\mathrm{GeV},\ p_T^{l_2} > 5\,\mathrm{GeV},\ 20^\circ < \theta^{l_{1,2}} < 150^\circ,\ Q^2 < 1\,\mathrm{GeV}^2,\ y < 0.82.$$

The cross sections are given at $\sqrt{s} = 318\,\mathrm{GeV}$: the small ($\sim 5\%$) correction needed for the 1996–97 data sample was extracted from the MC. The effect of final-state radiation on the cross section was checked and found to be negligible.

The total visible cross sections, corrected for acceptance, were measured to be

$$\sigma(\gamma\gamma \to e^+e^-) \;=\; 0.64 \pm 0.05^{+0.04}_{-0.03}\ \mathrm{pb} \tag{3}$$

for the electron channel, and

$$\sigma(\gamma\gamma \to \mu^+\mu^-) \;=\; 0.58 \pm 0.07^{+0.07}_{-0.06}\ \mathrm{pb} \tag{4}$$

for the muon channel.

Since the muon and electron cross sections differ only marginally, they were combined in a single measurement, evaluated as the weighted mean of the two [23], assuming the systematic uncertainties to be uncorrelated. The systematic uncertainties of each measurement were symmetrised before the combination, by taking as systematic uncertainty the largest between the negative and the positive. The total visible cross sections are shown in Table 4, compared with the SM predictions.

Differential cross sections as a function of the invariant mass, M_{12}, the transverse momentum of the highest-p_T lepton, $p_T^{l_1}$, and the scalar sum of the transverse momentum of the two leptons, $\sum p_T^l$, are shown in Fig. 5, separately for electrons and muons. The di-electron, di-muon and combined cross sections are summarised in Table 5. The combination was done as described for the total visible cross section. Good agreement is observed between the data and the SM predictions.

7 Conclusions

Events with two or more isolated leptons with high transverse momentum were observed using the full data sample taken with the ZEUS detector at HERA. The total number of multi-lepton events for different lepton configurations as well as their p_T and mass distributions were studied. No significant deviations from the predictions of the SM were observed. In addition, the total visible and differential cross sections for the e^+e^- and $\mu^+\mu^-$ signatures were measured in photoproduction and were observed to be in good agreement with the SM predictions.

8 Acknowledgements

We appreciate the contributions to the construction and maintenance of the ZEUS detector of many people who are not listed as authors. The HERA machine group and the DESY computing staff are especially acknowledged for their success in providing excellent operation of the collider and the data-analysis environment. We thank the DESY directorate for their strong support and encouragement.

References

[1] H1 Collaboration, F.D. Aaron et al., Phys. Lett. B 668 (2008) 268.

[2] ZEUS Collaboration, U. Holm (ed.), *The ZEUS Detector*. Status Report (unpublished), DESY (1993), available on `http://www-zeus.desy.de/bluebook/bluebook.html`.

[3] N. Harnew et al., Nucl. Inst. Meth. A 279 (1989) 290;
B. Foster et al., Nucl. Phys. Proc. Suppl. B 32 (1993) 181;
B. Foster et al., Nucl. Inst. Meth. A 338 (1994) 254.

[4] A. Polini et al., Nucl. Inst. Meth. A 581 (2007) 31.

[5] M. Derrick et al., Nucl. Inst. Meth. A 309 (1991) 77;
A. Andresen et al., Nucl. Inst. Meth. A 309 (1991) 101;
A. Caldwell et al., Nucl. Inst. Meth. A 321 (1992) 356;
A. Bernstein et al., Nucl. Inst. Meth. A 336 (1993) 23.

[6] G. Abbiendi et al., Nucl. Inst. Meth. A 333 (1993) 342.

[7] J. Andruszków et al., Preprint DESY-92-066, DESY, 1992.

[8] ZEUS Collaboration, M. Derrick et al., Z. Phys. C 63 (1994) 391.

[9] J. Andruszków et al., Acta Phys. Pol. B 32 (2001) 2025.

[10] M. Helbich et al., Nucl. Inst. Meth. A 565 (2006) 572.

[11] T. Abe, Comp. Phys. Comm. 136 (2001) 126.

[12] N. Arteaga-Romero, C. Carimalo and P. Kessler, Z. Phys. C 52 (1991) 289.

[13] H. Spiesberger, HERACLES *and* DJANGOH*: Event Generation for ep Interactions at HERA Including Radiative Processes*, 1998, available on `http://www.desy.de/~hspiesb/djangoh.html`.

[14] B. List and A. Mastroberardino, *Proc. Workshop on Monte Carlo Generators for HERA Physics*, p. 396. DESY, Hamburg, Germany (1999). Also in preprint DESY-PROC-1999-02, available on `http://www.desy.de/~heramc/`.

[15] T. Sjöstrand et al., Comp. Phys. Comm. 135 (2001) 238.

[16] R. Brun et al., GEANT3, Technical Report CERN-DD/EE/84-1, CERN, 1987.

[17] W.H. Smith, K. Tokushuku and L.W. Wiggers, *Proc. Computing in High-Energy Physics (CHEP), Annecy, France, Sept. 1992*, C. Verkerk and W. Wojcik (eds.), p. 222. CERN, Geneva, Switzerland (1992). Also in preprint DESY 92-150B.

[18] P.D. Allfrey et al., Nucl. Inst. Meth. A 580 (2007) 1257.

[19] ZEUS Collaboration, S. Chekanov et al., Eur. Phys. J. C 27 (2003) 173.

[20] ZEUS Collaboration, J. Breitweg et al., Eur. Phys. J. C 11 (1999) 427.

[21] M. Turcato. Ph.D. Thesis, Università degli Studi di Padova, Italy, Report DESY-THESIS-03-039, 2002.

[22] I. Marchesini. Diploma Thesis, Università degli Studi di Padova, Italy, 2007 (unpublished).

[23] CDF and DØ Collaboration, L. Demortier et al., FERMILAB-TM-2084 (1999).

ZEUS ($\mathcal{L} = 480\,\mathrm{pb}^{-1}$)

Topology	Data	Total SM	Multi-lepton Production	NC DIS	Compton
ee	545	563^{+29}_{-37}	429^{+21}_{-29}	74 ± 5	60 ± 10
$\mu\mu$	93	106±12	106±12	< 0.5	–
$e\mu$	46	42±4	37^{+3}_{-4}	4.5±1.2	–
eee	73	75^{+5}_{-4}	73^{+4}_{-5}	< 1	< 3
$e\mu\mu$	47	48±5	48±5	< 0.5	–
$eeee$	1	$0.9^{+0.5}_{-0.1}$	0.6±0.1	< 0.4	< 1
$ee\mu\mu$	2	$0.5^{+0.3}_{-0.1}$	0.4±0.1	< 0.5	–
All 4 leptons	3	$1.4^{+0.7}_{-0.1}$	1.0 ± 0.2	< 1.4	
ee ($\gamma\gamma$ sample)	166	$185^{+\ 8}_{-14}$	$183^{+\ 8}_{-14}$	1.4±1.0	1.4 ± 0.6
$\mu\mu$ ($\gamma\gamma$ sample)	72	$85^{+\ 9}_{-10}$	$85^{+\ 9}_{-10}$	< 0.5	–

Table 1: *The observed and predicted multi-lepton event yields for the ee, $\mu\mu$, $e\mu$, eee, $e\mu\mu$, eeee and $ee\mu\mu$ event topologies; the event yields for the ee and $\mu\mu$ topologies in the $\gamma\gamma$ samples. The quoted uncertainties consist of model uncertainties, MC statistical uncertainties and systematic experimental uncertainties added in quadrature. Limits at 95% C.L. are given when none or few events were selected from the background MC samples. The central value and the uncertainty on the total SM predictions are in these cases determined as explained in the text.*

ZEUS ($\mathcal{L} = 480\,\mathrm{pb}^{-1}$)

Topology, $M_{12} > 100\,\mathrm{GeV}$	Data	Total SM	Multi-lepton Production	NC DIS	Compton
ee	1	1.7 ± 0.2	0.9 ± 0.1	0.2 ± 0.1	0.6 ± 0.1
$\mu\mu$	0	0.4 ± 0.1	0.4 ± 0.1	< 0.01	–
$e\mu$	0	$0.06^{+0.03}_{-0.01}$	0.05 ± 0.02	< 0.02	–
eee	2	0.7 ± 0.1	0.7 ± 0.1	< 0.01	< 0.02
$e\mu\mu$	0	0.18 ± 0.05	0.18 ± 0.05	< 0.01	–

Table 2: *The observed and predicted high-mass, $M_{12} > 100\,GeV$, multi-lepton event yields. The invariant mass was calculated using the two highest-p_T leptons. The quoted uncertainties consist of model uncertainties, MC statistical uncertainties and systematic experimental uncertainties added in quadrature. Limits at 95% C.L. are given when none or few events were selected from the background MC samples. The central value and the uncertainty on the total SM predictions are in these cases determined as explained in the text.*

ZEUS ($\mathcal{L} = 480\,\mathrm{pb}^{-1}$)

$\sum p_T^l > 100\,\mathrm{GeV}$				
Data	Total SM	Multi-lepton Production	NC DIS	Compton
2	1.56 ± 0.15	1.16 ± 0.13	0.05 ± 0.02	0.35 ± 0.06

Table 3: *The observed and predicted high-$\sum p_T^l$ multi-lepton event yields for all topologies combined, where $\sum p_T^l$ was calculated using all the leptons in the event. The quoted uncertainties consist of model uncertainties, MC statistical uncertainties and systematic experimental uncertainties added in quadrature.*

ZEUS ($\mathcal{L} = 480\,\mathrm{pb}^{-1}$)

$\gamma\gamma$ sample	$\sigma_{\mathrm{DATA}}^{96-07}$ (pb)	σ_{SM} (pb)
ee	$0.64 \pm 0.05^{+0.04}_{-0.03}$	0.71 ± 0.02
$\mu\mu$	$0.59 \pm 0.07^{+0.07}_{-0.06}$	0.69 ± 0.02
Combined	$0.63 \pm 0.04 \pm 0.03$	0.70 ± 0.02

Table 4: *Total cross section for $\gamma\gamma \to ee$ and $\gamma\gamma \to \mu\mu$ samples, combined as explained in the text, compared with the predictions from the* Grape *MC.*

ZEUS ($\mathcal{L} = 480\,\mathrm{pb}^{-1}$)

Bin (GeV)	$\sigma^{96-07}_{\mathrm{DATA}}$ (fb/ GeV)			σ_{SM} (fb/ GeV)
	e^+e^-	$\mu^+\mu^-$	Combined	
$15 < M_{12} < 25$	$23.0 \pm 3.2\ ^{+1.6}_{-1.2}$	$32.7 \pm 5.0\ ^{+3.7}_{-3.2}$	$25.4 \pm 2.7 \pm 1.5$	30.4 ± 1.0
$25 < M_{12} < 40$	$19.1 \pm 2.0\ ^{+1.6}_{-1.2}$	$12.6 \pm 2.6\ ^{+1.4}_{-1.3}$	$16.3 \pm 1.6 \pm 1.1$	19.8 ± 0.7
$40 < M_{12} < 60$	$3.8 \pm 0.8\ ^{+0.3}_{-0.4}$	$2.5 \pm 1.0\ ^{+0.3}_{-0.3}$	$3.3 \pm 0.6 \pm 0.3$	3.0 ± 0.1
$60 < M_{12} < 100$	$0.15 \pm 0.11\ ^{+0.04}_{-0.03}$	$0.21 \pm 0.21\ ^{+0.03}_{-0.02}$	$0.17 \pm 0.10 \pm 0.03$	0.26 ± 0.02
$10 < p_T^{l_1} < 15$	$90.7 \pm 8.4^{+6.1}_{-2.5}$	$94 \pm 12^{+11}_{-9}$	$91.6 \pm 6.9 \pm 5.3$	103.2 ± 3.3
$15 < p_T^{l_1} < 20$	$26.4 \pm 4.3^{+2.2}_{-1.8}$	$10.7 \pm 4.4^{+1.3}_{-1.1}$	$18.1 \pm 3.1 \pm 1.3$	23.7 ± 0.9
$20 < p_T^{l_1} < 25$	$4.2 \pm 1.7^{+0.8}_{-0.5}$	$8.9 \pm 4.0^{+1.0}_{-0.9}$	$5.0 \pm 1.6 \pm 0.7$	7.3 ± 0.4
$25 < p_T^{l_1} < 50$	$0.90 \pm 0.37^{+0.08}_{-0.11}$	$0.70 \pm 0.50^{+0.08}_{-0.08}$	$0.82 \pm 0.29 \pm 0.08$	0.88 ± 0.06
$15 < \sum p_T^l < 25$	$36.7 \pm 4.0^{+2.4}_{-1.3}$	$38.4 \pm 5.5^{+4.4}_{-3.9}$	$37.2 \pm 3.2 \pm 2.2$	43.9 ± 1.4
$25 < \sum p_T^l < 40$	$15.8 \pm 1.9^{+1.3}_{-1.1}$	$11.2 \pm 2.6^{+1.3}_{-1.1}$	$14.0 \pm 1.5 \pm 0.9$	14.6 ± 0.5
$40 < \sum p_T^l < 60$	$1.24 \pm 0.44^{+0.21}_{-0.17}$	$1.32 \pm 0.76^{+0.15}_{-0.14}$	$1.26 \pm 0.38 \pm 0.16$	1.69 ± 0.11
$60 < \sum p_T^l < 100$	$0.092 \pm 0.092^{+0.021}_{-0.024}$	$0.18 \pm 0.18^{+0.02}_{-0.02}$	$0.11 \pm 0.08 \pm 0.02$	0.16 ± 0.02

Table 5: *Differential cross section as a function of the invariant mass, M_{12}, the transverse momentum of the highest-p_T lepton, $p_T^{l_1}$, and the scalar sum of the transverse momentum of the two leptons, $\sum p_T^l$, for di-lepton events in the kinematic region defined in the text, compared with the predictions from the* GRAPE *Monte Carlo. The results are shown separately for the ee and $\mu\mu$ samples, as well as for the combined sample.*

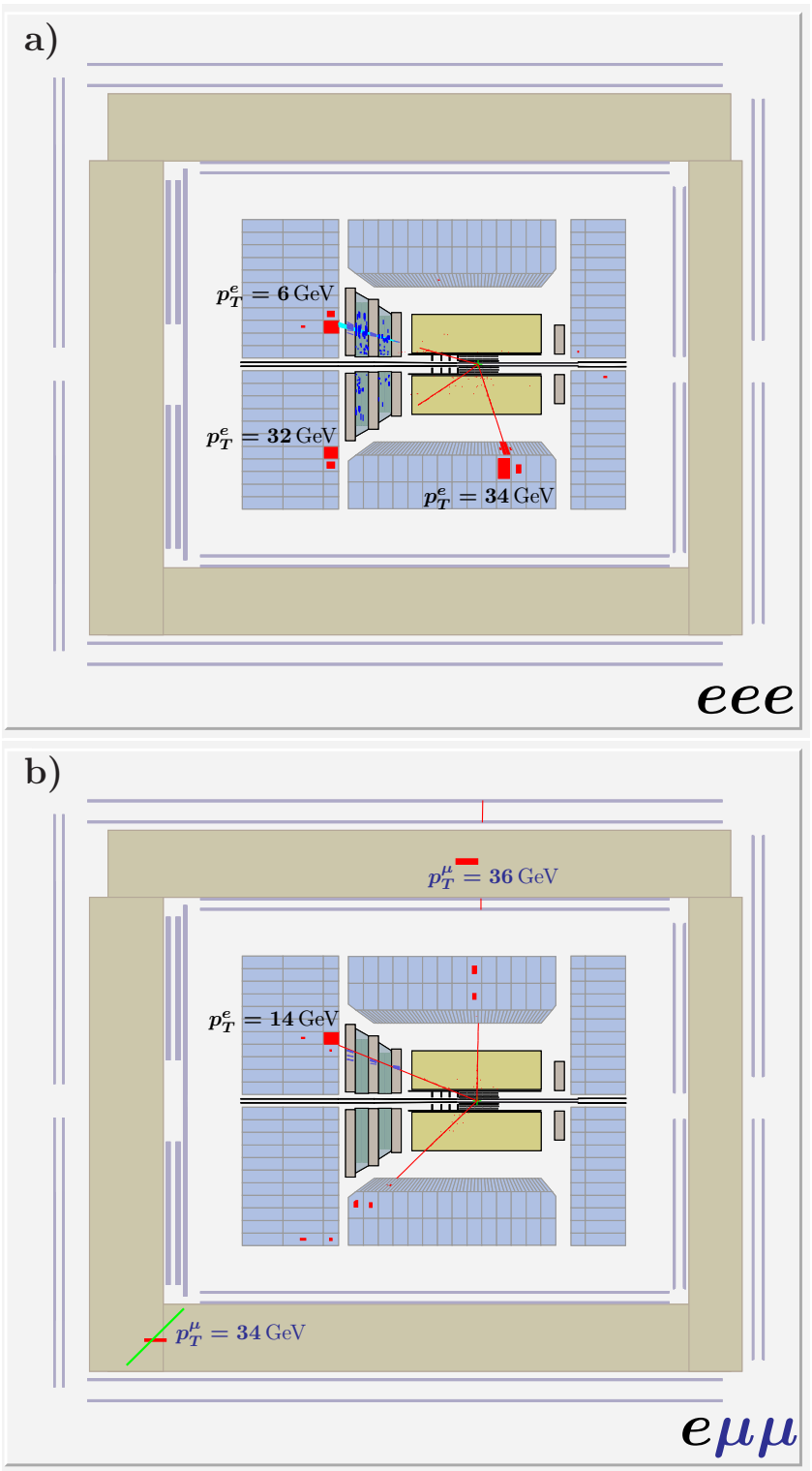

Figure 1: *a) An event with three electron candidates in the ZEUS detector. The invariant mass of the two highest-p_T electrons is $M_{12} = 113$ GeV; the corresponding transverse momenta are given above. b) An event with two muons and an electron candidate in the ZEUS detector. The invariant mass of the di-muon pair is 77.5 GeV; the corresponding transverse momenta are given above.*

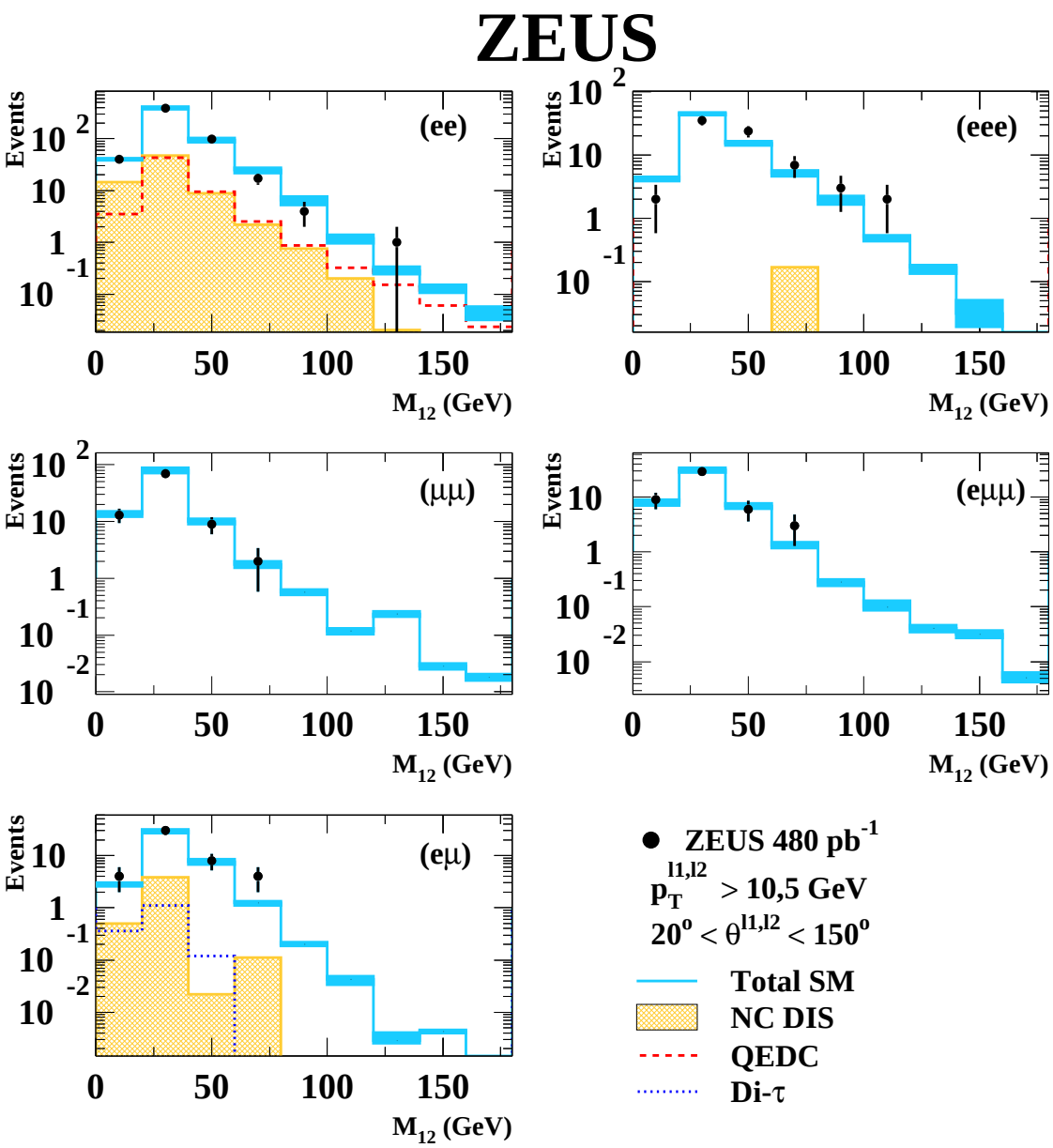

Figure 2: *Distributions of the invariant mass of the two highest-p_T leptons for the different multi-lepton topologies: ee, eee, μμ, eμμ, eμ. The ZEUS data are displayed as the full dots. The errors on the data are given by the square root of the number of events in each bin. The SM predictions are represented as the solid line and are obtained by summing the contributions of di-lepton production, NC DIS, QED Compton events, and, for the eμ channel, di-tau production. The error band represents the systematic uncertainty on the SM predictions.*

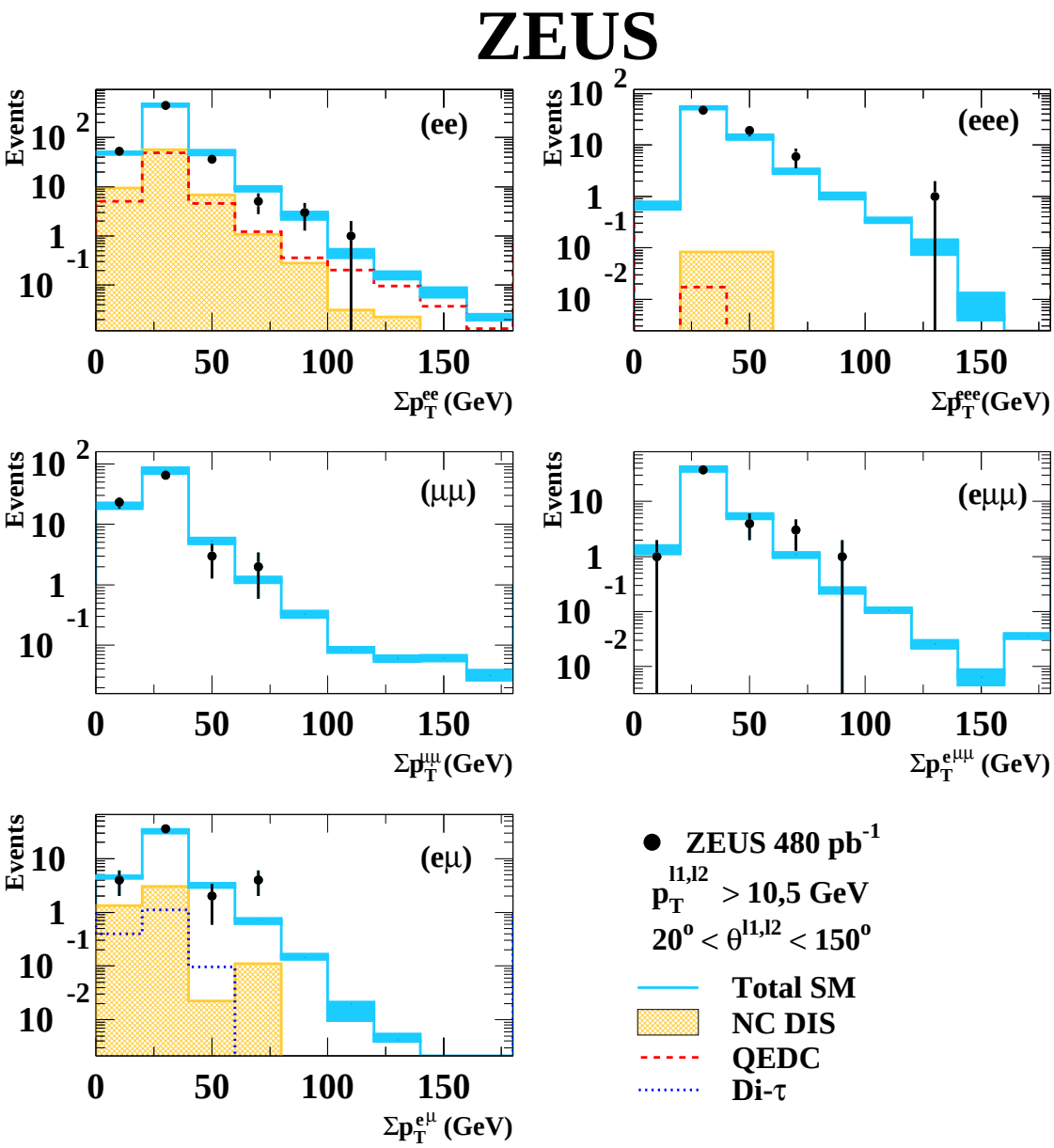

Figure 3: *Distributions of the sum of the transverse momenta of the leptons for the different multi-lepton topologies: ee, eee, μμ, eμμ, eμ. The ZEUS data are displayed as the full dots. The errors on the data are given by the square root of the number of events in each bin. The SM predictions are represented as the solid line and are obtained by summing the contributions of di-lepton production, NC DIS, QED Compton events, and, for the eμ channel, di-tau production. The error band represents the systematic uncertainty on the SM predictions.*

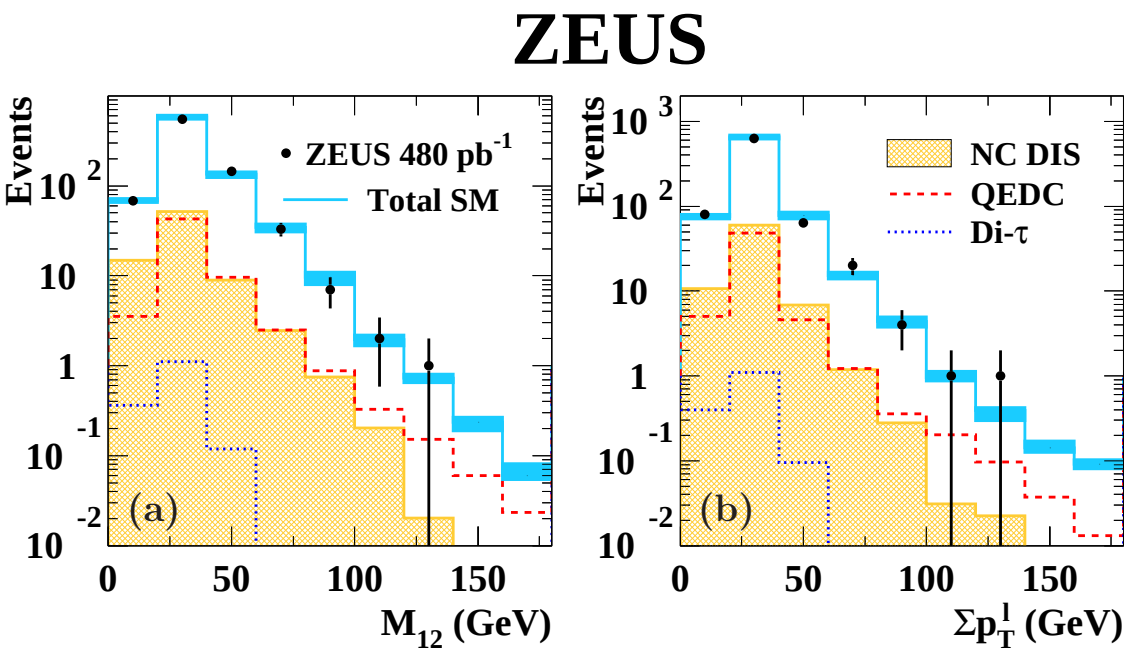

Figure 4: *Distributions of (a) the invariant mass of the two highest-p_T leptons and (b) the sum of the transverse momenta of the leptons for all the individual lepton topologies combined: ee, eee, μμ, eμμ, eμ. The ZEUS data are displayed as the full dots. The errors on the data are given by the square root of the number of events in each bin. The SM predictions are represented as the solid line and are obtained by summing the contributions of di-lepton production, NC DIS, QED Compton events, and, for the eμ channel, di-tau production. The error band represents the systematic uncertainty on the SM predictions.*

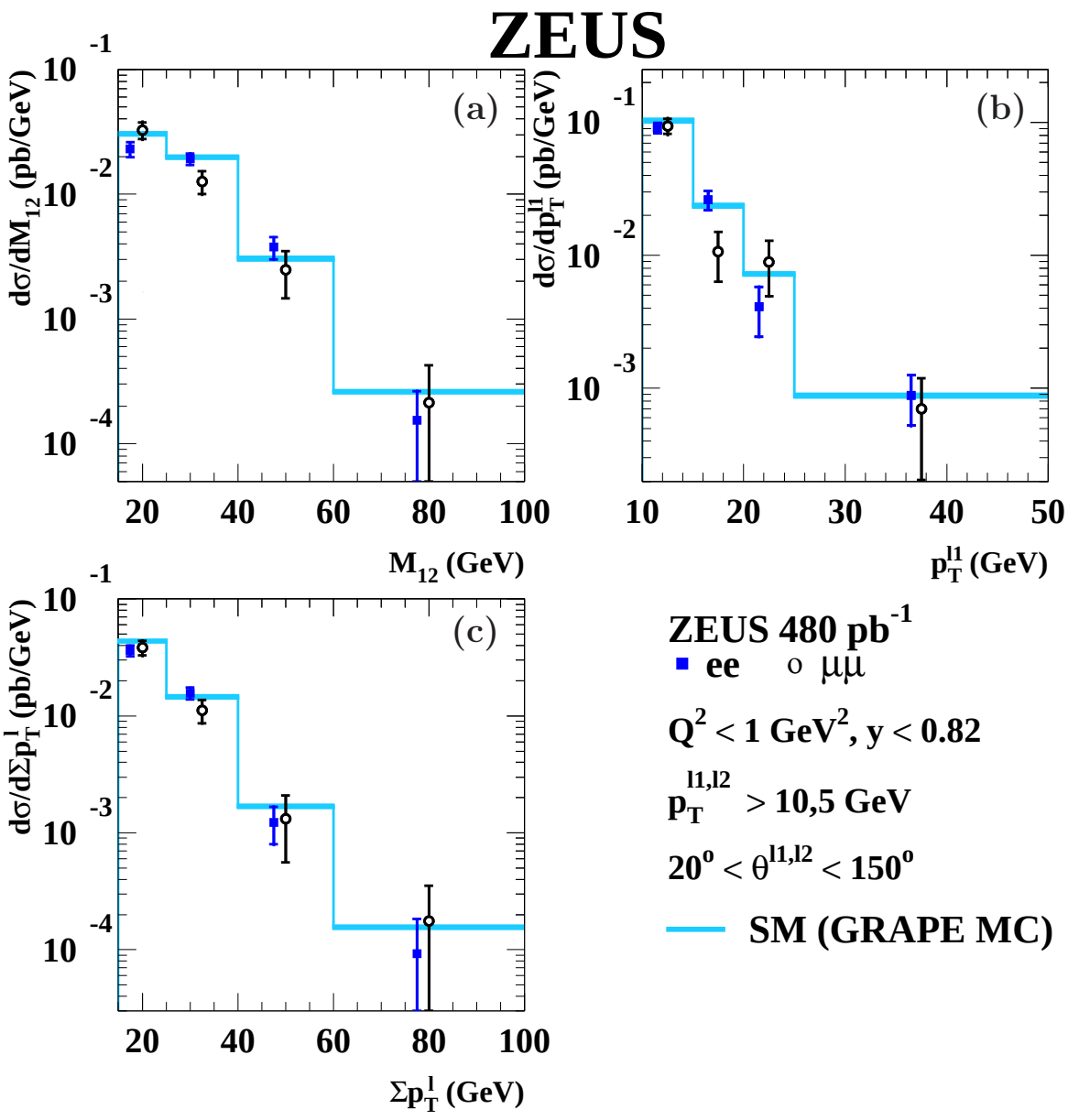

Figure 5: *Differential cross sections as a function of (a) the invariant mass of the lepton pair, M_{12}, (b) the transverse momentum $p_T^{l_1}$ of the highest-p_T lepton, and (c) the scalar sum of the transverse momenta of the two highest-p_T leptons, $\sum p_T^l$. The di-muon cross sections are shown as the open dots, while the full dots are the di-electron measurements, which have been displaced for clarity. The data are compared with the predictions of the* GRAPE *Monte Carlo. The full error bars are the quadratic sum of the statistical (inner part) and systematic uncertainties.*